

On the Large Eddy Simulation of High Prandtl Number Scalar Transport Using Dynamic Subgrid-Scale Model

Yang Na*

Center for Multidisciplinary Aerospace System Design, Department of Mechanical Engineering,
Konkuk University, Seoul 143-701, Korea

The present study investigates passive scalar transport using an eddy viscosity/diffusivity model in turbulent channel flow with Prandtl number range 1-10. Dynamic subgrid-scale model (DSM) was applied to the transport equation for passive scalar to determine the eddy diffusivity dynamically. To assess the feasibility of the DSM model applied for passive scalar, *a priori* test on direct numerical simulation data was conducted and the results are compared with those obtained from a large eddy simulation that uses DSM model *a posteriori*. As the Prandtl number increases, the discrepancy in subgrid-scale (SGS) heat flux amplifies but the shape of SGS temperature dissipation profiles shows reasonable agreement. This suggests that energy transfer between resolved and subgrid-scales are reasonably predicted regardless of the accuracy in SGS heat flux vectors. While *a priori* test shows that SGS turbulent Prandtl number changes significantly with Prandtl number, the actual LES results are found to be insensitive to Prandtl number away from the wall. Thus, the DSM model has some limitations in the prediction of high Prandtl number flows.

Key Words : Prandtl Number, Passive Scalar, Turbulent Flow, SGS Heat Flux, SGS Dissipation, Direct Numerical Simulation, Large Eddy Simulation

Nomenclature

Roman Symbols

C : Model coefficient for eddy viscosity in DSM model
 C_T : Model coefficient for eddy diffusivity in DSM model
 Pr : Prandtl number
 Pr_t : Turbulent Prandtl number
 $Pr_{t,SGS}$: Subgrid-scale turbulent Prandtl number
 q_k : Subgrid-scale heat flux vector ($k=1, 2, 3$)
 Re_τ : Reynolds number based on friction velocity and half channel height
 S_{ij} : Strain rate tensor ($i, j=1, 2, 3$)
 T : Temperature
 T_{rms} : Root-mean square temperature

T_w : Wall temperature
 t : time
 u_i : Velocity component in Cartesian coordinate ($i=1, 2, 3$)
 u, v, w : Streamwise, wall-normal, spanwise velocity components
 x_i : Cartesian coordinate ($i=1, 2, 3$)
 x, y, z : Cartesian coordinate in streamwise, wall-normal and spanwise directions

Greek Symbols

α : Molecular diffusivity
 α_t : Eddy diffusivity
 $\bar{\Delta}$: Grid filter width
 $\hat{\Delta}$: Test filter width
 ε_τ : Subgrid-scale dissipation
 ε_q : Subgrid-scale temperature dissipation
 τ_{ij} : Subgrid-scale residual stress tensor ($i, j=1, 2, 3$)
 ν : Kinematic viscosity
 ν_t : Eddy viscosity

* E-mail : yangna@konkuk.ac.kr

TEL : +82-2-450-3467; FAX : +82-2-447-5886

Department of Mechanical Engineering, Konkuk University, Seoul 143-701, Korea. (Manuscript Received April 2, 2003; Revised November 24, 2003)

Superscript

()⁺ : Nondimensional variable in wall units

1. Introduction

In large-eddy simulation (LES) the effect of large, energy-containing scales is directly computed and the small subgrid-scales (SGS) are modelled based on the assumption that small scales are nearly homogeneous and isotropic. The most commonly used SGS stress model, the dynamic eddy viscosity model (Germano et al, 1991), is capable of backscatter and has been successfully applied to various types of turbulent flows including turbulent mixing and transitional flows (Vreman et al, 1997; Piomelli et al, 1991).

For a better design of various type of thermal engineering applications, less computationally intensive yet still accurate prediction methods for temperature fields are desirable but there has been significantly less effort in LES modeling studies for passive scalar than for velocity field. An earlier work of Cabot and Moin (1993) was devoted to the formulation of the dynamic subgrid-scale model (DSM) for incompressible scalar transport using an eddy viscosity/diffusivity approach but their study was limited to low Prandtl numbers. Even though their work showed a good possibility of applying the DSM to temperature field, detailed analysis regarding SGS energy transfer in temperature field was not attempted to justify their reasonable success. Several previous LES works involving passive scalar were confined to low Prandtl number flows (e.g. Pr=0.71) where 'Reynolds analogy' generally holds.

The present work is motivated by the need for SGS data for passive scalar with high Prandtl number (up to 10) to understand the physical process in energy transfer of passive scalar at the SGS level to support the LES modeling development. To gain a better understanding of the residual heat flux and temperature dissipation, the technique known as an *a priori* test by Clark, Ferziger and Reynolds (1979) was applied to the direction numerical simulation (DNS) data for channel flow with Pr=1, 3 and 10. Also, LES

that uses DSM was performed *a posteriori* for the same Prandtl numbers.

2. Methodology

2.1 DSM model for passive scalar

By applying the grid filter, one obtains the filtered governing equations for the LES of a passive scalar in an incompressible flow :

$$\frac{\partial \bar{u}_i}{\partial x_i} = 0 \quad (1)$$

$$\begin{aligned} \frac{\partial \bar{u}_i}{\partial t} + \frac{\partial}{\partial x_j} (\bar{u}_i \bar{u}_j) \\ = -\frac{1}{\rho} \frac{\partial \bar{p}}{\partial x_i} + \frac{\partial}{\partial x_j} (2\nu \bar{S}_{ij} - \tau_{ij}) \end{aligned} \quad (2)$$

$$\frac{\partial \bar{T}}{\partial t} + \frac{\partial}{\partial x_k} (\bar{T} \bar{u}_k) = \frac{\partial}{\partial x_k} \left(\alpha \frac{\partial \bar{T}}{\partial x_k} - q_k \right) \quad (3)$$

where the grid filtering operation is denoted by an overbar. The filtered strain rate tensor \bar{S}_{ij} is defined by

$$\bar{S}_{ij} \equiv \frac{1}{2} \left(\frac{\partial \bar{u}_i}{\partial x_j} + \frac{\partial \bar{u}_j}{\partial x_i} \right) \quad (4)$$

The effects of small scales appear in the residual SGS stress, τ_{ij} , and heat flux, q_k , terms which must be modeled as

$$\tau_{ij} = \bar{u}_i \bar{u}_j - \bar{u}_i \bar{u}_j \quad (5)$$

$$q_k = \bar{T} \bar{u}_k - \bar{T} \bar{u}_k \quad (6)$$

The dynamic eddy viscosity model parameterizes the anisotropic part of the SGS stress by an eddy viscosity assumption

$$\tau_{ij} - \frac{1}{3} \delta_{ij} \tau_{kk} = -2\nu_t \bar{S}_{ij}, \quad \nu_t = C \bar{\Delta}^2 |\bar{S}| \quad (7)$$

and analogous eddy diffusivity model was suggested by Erlebacher, Hussaini, Speziale and Zang (1990)

$$q_k = -\alpha_t \frac{\partial \bar{T}}{\partial x_k}, \quad \alpha_t = C_T \bar{\Delta}^2 |\bar{S}| \quad (8)$$

where the coefficients C and C_T are calculated dynamically during the simulation. Here, $\bar{\Delta}$ denotes the grid filter width and is related to the mesh size of the resolved field. Thus, the LES results depend on $\bar{\Delta}$. The definition of $|\bar{S}|$ is given as follows :

$$|\bar{S}| \equiv |2\bar{S}_{ij} \bar{S}_{ij}|^{\frac{1}{2}} \quad (9)$$

The key element of the DSM concept is the utilization of the data contained in the resolved field. This information is brought by introducing a test filter (or high-pass filter), which generates a flow field with scales larger than the resolved field. By applying a test filter, residual stress and scalar flux are defined by

$$T_{ij} = \widehat{u_i u_j} - \widehat{u_i} \widehat{u_j} \quad (10)$$

$$Q_k = \widehat{T u_k} - \widehat{T} \widehat{u_k} \quad (11)$$

where the circumflex denotes the test filtering process.

In a manner similar to equations (7)-(8), T_{ij} and Q_k are modelled at the test filter level.

$$T_{ij} - \frac{1}{3} \delta_{ij} T_{kk} = 2 \hat{\nu}_t \widehat{S}_{ij}, \quad \hat{\nu}_t = C \widehat{\Delta}^2 |\widehat{S}| \quad (12)$$

$$Q_k = -\alpha_t \frac{\partial \widehat{T}}{\partial x_k}, \quad \alpha_t = C_T \widehat{\Delta}^2 |\widehat{S}| \quad (13)$$

where $|\widehat{S}|$ is defined similar to equation (9) and $\widehat{\Delta}$ is the width of the test filter. Using Germano's identity, the difference between $T_{ij} - \hat{\tau}_{ij}$ and $Q_k - \hat{q}_k$ can be directly calculated from the resolved field.

$$L_{ij} = T_{ij} - \hat{\tau}_{ij} = \widehat{u_i u_j} - \widehat{u_i} \widehat{u_j} \quad (14)$$

$$F_k = Q_k - \hat{q}_k = \widehat{T u_k} - \widehat{T} \widehat{u_k} \quad (15)$$

Substituting the eddy viscosity/diffusivity model into equations (14)-(15), coefficients C and C_T are determined from

$$L_{ij} - \frac{1}{3} \delta_{ij} L_{kk} = -C \widehat{\Delta}^2 M_{ij}, \quad M_{ij} = 2[(\widehat{\Delta}/\Delta)^2 |\widehat{S}| \widehat{S}_{ij} - |\widehat{S}| \widehat{S}_{ij}] \quad (16)$$

$$F_k = -C_T \widehat{\Delta}^2 H_k, \quad H_k = (\widehat{\Delta}/\Delta)^2 |\widehat{S}| \frac{\partial \widehat{T}}{\partial x_k} - |\widehat{S}| \frac{\partial \widehat{T}}{\partial x_k} \quad (17)$$

There are several proposed ways of obtaining coefficients C and C_T but many studies (Germano et al, 1991; Cabot and Moin, 1993) suggest that Lilly's (1992) least squares analysis on equations (16)-(17) gives the better results. This procedure is equivalent to contracting equations (16)-(17) with M_{ij} and H_k , respectively as follows:

$$C = \frac{1}{2} \frac{M_{ij} L_{ij}}{M_{ki} M_{kl}}, \quad C_T = -\frac{F_k H_k}{H_i H_i} \quad (18)$$

The quantities in denominators of equation (18) can become zero, which would make the coefficients C and C_T ill-conditioned. Germano et al. (1991) showed that this is indeed the case in turbulent channel flow. Therefore, it was assumed that C and C_T are only a function of y and t and the average of both numerator and denominator is taken over a homogeneous plane parallel to the wall to alleviate the numerical instability.

2.2 A priori test using filtered DNS data

An *a priori* test on the dynamic SGS model (8) was carried out to determine the accuracy with which the model predicts the SGS heat flux and temperature dissipation. The test was performed using the DNS database of Na et al. (1999) for turbulent channel flow where the walls are maintained at two different constant temperatures. The Prandtl number varies from 1 to 10. The Reynolds number based on friction velocity and half channel height, Re_τ , is 150 and the computational domain size in wall unit is $1900 \times 300 \times 950$ in the x , y and z directions, respectively. The DNS results for $Pr=1$ and 3 were obtained for a $128 \times 129 \times 128$ grid for which Δy^+ varied from 0.045 to 3.68. The resolution in the x and z directions were $\Delta x^+ = 15$, $\Delta z^+ = 7.5$. The DNS results for $Pr=10$ are for an x , y , z grid of $128 \times 193 \times 128$ and the resolution in the y -direction varied from $\Delta y^+ = 0.02$ at the wall to $\Delta y^+ = 2.45$ at the center of the channel.

Although the velocity and temperature fields were available both in Fourier and physical spaces, all the filtering related operations were performed in the physical space using a box filter (with trapezoidal rule). Thus, the exact values of SGS stress τ_{ij} , SGS heat flux q_k and SGS temperature dissipation, $\varepsilon_q = q_k \frac{\partial T}{\partial x_k}$ were directly calculated by filtering the DNS data using a box filter (via equations (5) and (6)) and the results of *a priori* test were obtained by solving the equation (8) using the filtered DNS field. The width of the filter is given by $\bar{\Delta}_x = 2\Delta_x$, $\bar{\Delta}_z = 2\Delta_z$ in the streamwise and spanwise directions, re-

spectively. No explicit filtering was applied in the wall-normal directions. One of the reasons of this choice of box filter is for the purpose of comparison with those of LES that uses a finite difference method with inflow/outflow boundary conditions. Germano et al. (1991) performed a similar analysis in Fourier space for the velocity field and suggested that it would be worth evaluating the performance of DSM by comparing the exact values of the model with the results from an *a priori* test as well as with those of an actual LES (explained in section 2.3) conducted in a physical space. The underlined motivation for their suggestion is to investigate properties of DSM used with different filters other than the sharp cutoff filter they tried. In the present work, this idea was extended to the operation of temperature field in addition to the velocity field and the performance of DSM is checked by processing the data in physical space using a box filter. And the results are compared with those obtained from an actual LES that uses the same box filter.

All the results from *a priori* test were obtained by averaging the flow field in time for about $200 \nu/u_\tau^2$. Usually this period of time may not be enough to get very smooth statistics, but in the light of the purpose of *a priori* test, it is thought to be reasonably sufficient judging from the result of Germano et al. (1991).

2.3 LES with DSM

In order to determine the validity of the dynamic SGS model (8), it was also tested *a posteriori* by conducting an LES. For the present LES of channel flow, the computational domain size, temperature boundary condition and the Reynolds number were set equal to those of DNS as given in section 2.1.

The governing equations described in section 2.2 are integrated in time using a semi-implicit scheme. A low-storage three-substep, third order Runge-Kutta scheme (Spalart et al., 1991) is used for treating convective terms explicitly and a second order Crank-Nicolson scheme is used for treating viscous terms implicitly. All spatial derivatives are approximated with second order central difference scheme except for the convective

term for temperature in which QUICK scheme is employed to prevent the numerical oscillation.

The flow is assumed to be homogeneous in the spanwise direction, justifying the use of periodic boundary conditions in that direction. The widely-used convective boundary condition was applied at exit. For the generation of inflow turbulence, the (y - z) plane far downstream from the inlet (located approximately $0.85L_x$ downstream from the inlet) has been fed continuously into the inlet plane. In doing so, the location of this plane is assumed to be sufficiently decorrelated from the inlet (since this plane is about $0.85L_x$ or equivalently 1600 in wall unit apart from the inlet) and to be practically free from any significant disturbances associated with convective boundary condition (since it is about $0.15L_x$ apart from the exit). Since all the statistics were calculated using the planes only up to $x/L_x=0.85$, this way of generating inflow turbulence is believed to be, in effect, equivalent to imposing the periodic boundary condition in the streamwise direction and this justifies a direct comparison of LES results with those of DNS obtained with periodic boundary conditions.

As in the *a priori* test done on a DNS database, the box filter was applied as both grid and test filters in the streamwise and spanwise directions but no explicit filtering was done in the normal direction. The only adjustable parameter is the ratio of $\hat{\Delta}_i/\bar{\Delta}_i$. Several previous studies (Germano et al., 1991; Cabot and Moin, 1993) suggest that the choice of the ratio $\hat{\Delta}_i/\bar{\Delta}_i=2$ was found to yield the best results and the actual LES with dynamic model appear to be very insensitive to this ratio. Thus, the value of 2 was chosen for the present study.

A grid of $64 \times 65 \times 64$ was used for $Pr=1$ and 3 computations and a grid of $97 \times 97 \times 97$ for the $Pr=10$ and all the statistics were averaged over a period of $600\nu/u_\tau^2$. Fig. 1 shows the comparison of mean and rms temperature profiles obtained with three different resolutions for $Pr=1$. As Cabot and Moin (1993) indicated, DSM is generally too dissipative and tends to underpredict the eddy viscosity as well as diffusivity and this in turn results in a higher prediction of mean and

rms temperatures than those obtained from the filtered DNS. Fig. 1 also shows that the agreement gets improved in a consistent way as the resolution gets better but the amount of improvement decreases sharply as the resolution increases. Thus, the gain which will be obtained from a higher resolution is thought to be limited. Ghosal (1996) showed that numerical errors (both aliasing and truncation errors) can deteriorate the SGS terms in the numerical simulations of homogeneous isotropic turbulence with low order finite difference approximation. Even though no theoretical framework for quantifying the errors in the general nonlinear turbulent flows exist at present, at least a consistency of reduction of errors with increasing the resolution can be

established in Fig. 1. This result would indicate that truncation errors did not significantly pollute the SGS terms and the truncation error can be controlled by using a higher resolution. And the results obtained with $65 \times 65 \times 65$ grids are believed to be sufficiently good enough for the purpose of discussion given in section 3. Although the results for $Pr=3$ are not presented here, a very similar trend was found and the same number of grid points was used for the computation.

Figure 2 shows the LES results for $Pr=10$ with three different resolutions. As the Prandtl number becomes larger, more grid points will be required since the temperature field with higher Prandtl number will generate a wider range of length

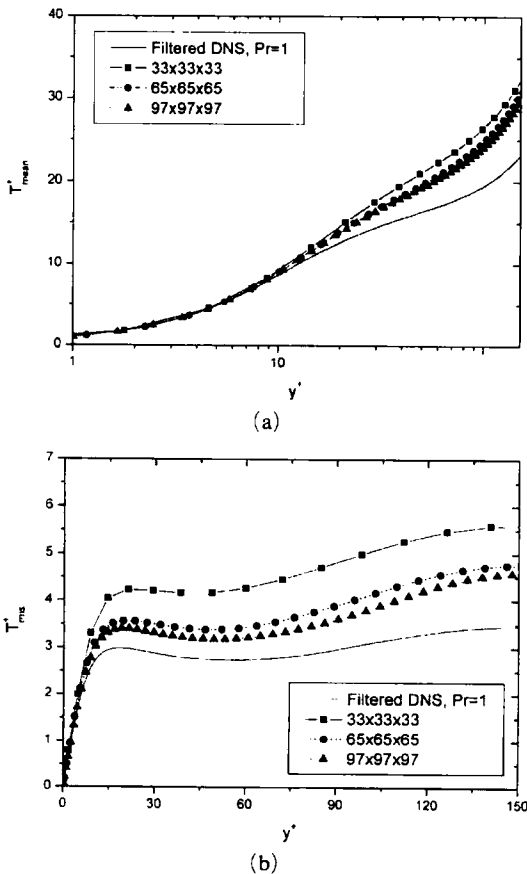


Fig. 1 Mean and rms temperature profiles for $Pr=1$ obtained with different resolutions. (a) Mean temperature; (b) rms temperature

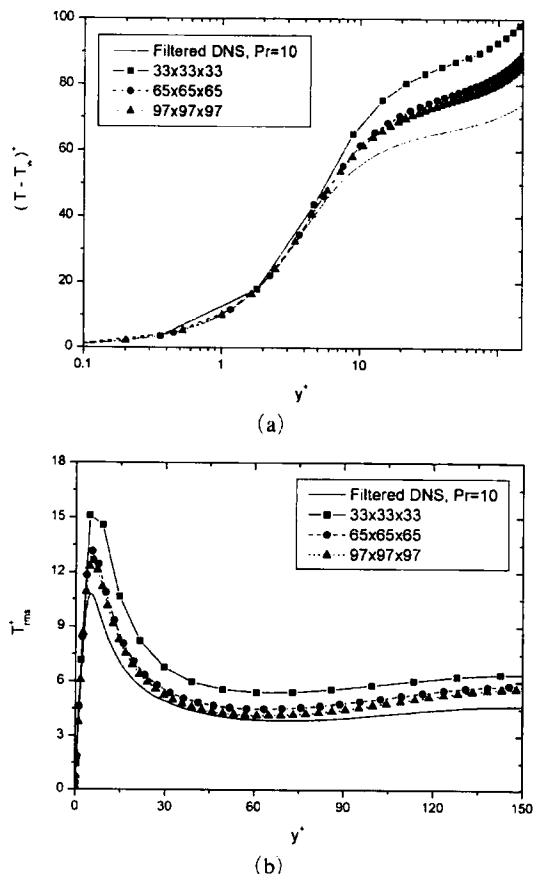


Fig. 2 Mean and rms temperature profiles for $Pr=10$ obtained with different resolutions. (a) Mean temperature; (b) rms temperature

scales and thus, a study regarding a proper resolution for $Pr=10$ should be established. Fig. 2 again shows the same conclusion that the better agreement is obtained with a higher resolution. Since the QUICK scheme was incorporated in solving the equation (3), temperature fluctuations are subject to damping and this fact should be taken care of when interpreting the rms results for high Prandtl number flows. Judging from the fact that the amount of improvement decreases sharply as the resolution increases, it was decided that a grid of $97 \times 97 \times 97$ is sufficient for $Pr=10$ for the purpose of comparison with the filtered DNS results. A complete resolution study which will include an investigation about the relationship between energy distribution in wavenumber space and the box filter width will remain as a future work.

3. Results

A principal focus of the paper is the comparison of SGS heat flux and temperature dissipation obtained from *a priori* test with the exact values and those from an LES test *a posteriori* in order to determine the accuracy with which the equation (8) predicts the SGS heat flux and temperature dissipation for high Prandtl number flows.

Figure 3 is a comparison of mean temperature profiles obtained from a filtered DNS and LES for $Pr=1, 3$ and 10 , showing larger discrepan-

cies at progressively larger Pr . Cabot and Moin (1993) also found that the mean streamwise velocity and temperature profiles from LES are consistently higher than those from DNS by analyzing the DNS results of both Kim et al. (1989) for $Pr=0.1, 0.71, 2$ and Kasagi et al. (1992) for $Pr=0.71$. This is probably caused by the underprediction of wall shear velocity from the LES regardless of the filter type used since the DSM is generally believed to be too dissipative at least for low Reynolds number simulations. It is noted that the slopes of the temperature profiles are approximated constant for all the Prandtl numbers considered but are lower than the value of 0.48 obtained by Subramanian and Antonia (1981). This difference in slope is thought to be due to the different thermal boundary condition imposed at the wall and the much lower Reynolds number considered in the present work.

Figure 4 represents calculations of the root mean-square of temperature. Maxima correspond roughly to the maxima in the production of temperature fluctuations (Na et al., 1999). Both LES and filtered DNS results show reasonable agreement of the locations of maxima for all the Prandtl numbers. Again, LES results predict higher energy in temperature fluctuations for all the Prandtl numbers. In the present flow configuration, the mean temperature gradient in the middle of the channel remains finite due to the constant

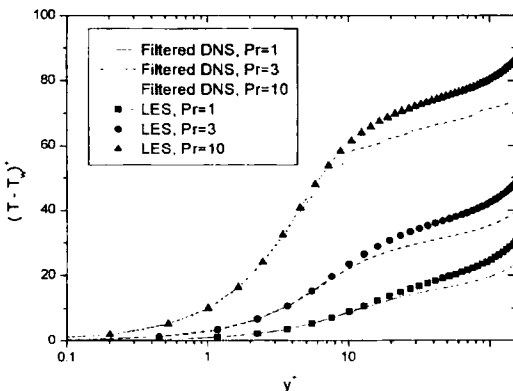


Fig. 3 Mean temperature profiles in semi-log. coordinate for $Pr=1, 3$ and 10

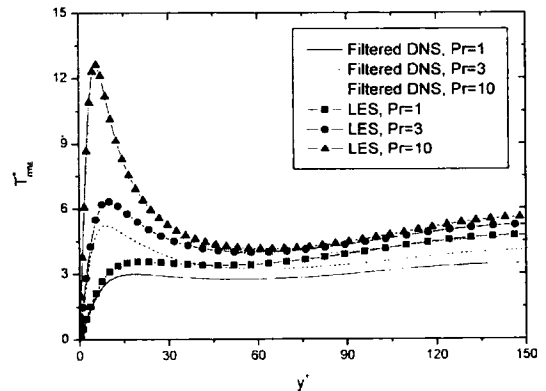


Fig. 4 Root-mean square temperature profiles for $Pr=1, 3$ and 10

wall temperature boundary condition as opposed to the mean streamwise velocity and, thus, the temperature fluctuations remains finite there and are significantly higher than velocity fluctuations.

In Fig. 5, the mean SGS shear stress $\langle \tau_{12} \rangle$ and dissipation $\langle \varepsilon_\tau \rangle$ are compared. Exact values are directly extracted from the DNS database using the equation (5). As mentioned in section 2.2, the result of *a priori* test was obtained by solving the equation (7) using the filtered DNS field. Although the magnitudes are not predicted correctly, all the curves present very similar shapes. The LES results underestimated both $\langle \tau_{12} \rangle$ and $\langle \varepsilon_q \rangle$ and this indicates that the current model is over dissipative given the present resolution and

filter ratio.

The mean SGS heat flux $\langle q_2 \rangle$ is shown in Fig. 6. As in SGS shear stress $\langle \tau_{12} \rangle$ the LES predictions are lower than the exact values. As the

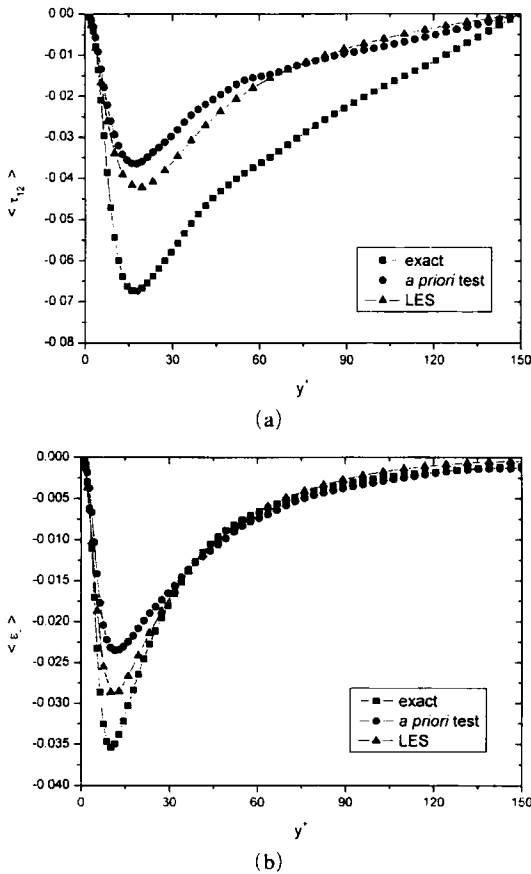


Fig. 5 Plane-averaged subgrid-scale shear stress $\langle \tau_{12} \rangle$ and dissipation $\langle \varepsilon_\tau \rangle$ for $Re_\tau=150$ turbulent channel flow. (a) SGS shear stress ; (b) Dissipation

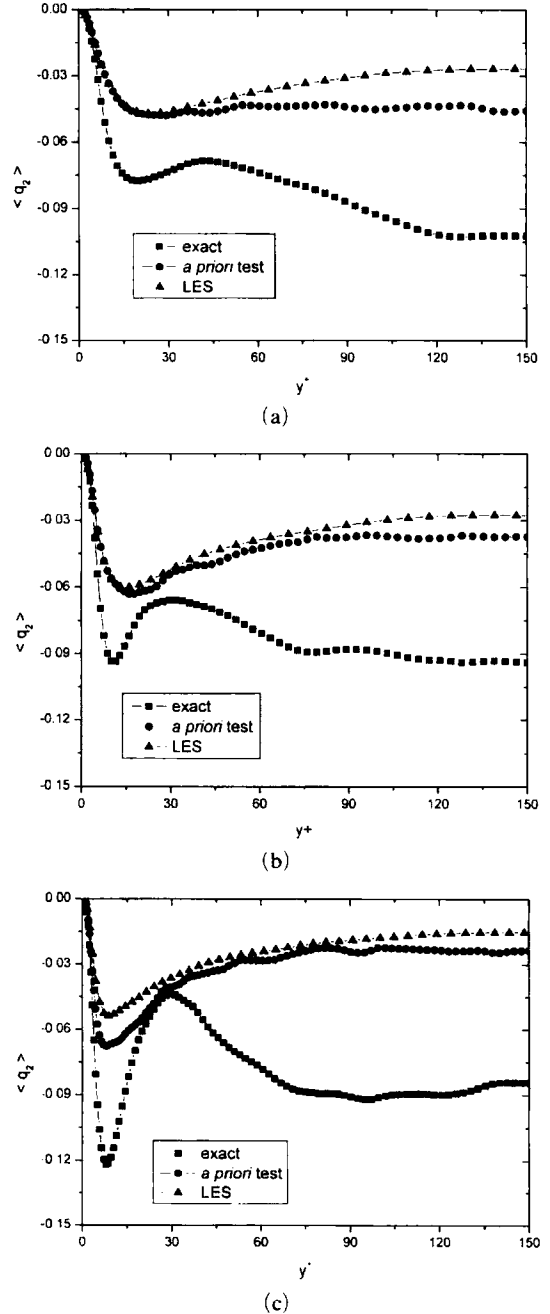


Fig. 6 Plane-averaged subgrid-scale heat flux, $\langle q_2 \rangle$. (a) $Pr=1$; (b) $Pr=3$; (c) $Pr=10$

Prandtl number increases, near-wall peak of exact values gets more pronounced similar to the behavior of T_{rms} shown in Fig. 4. While the SGS contribution to the energy and turbulent heat flux is relatively small for low Prandtl numbers, it becomes increasingly important for higher Prandtl number flows. Thus, the noticeable discrepancy shown for $Pr=10$ is very disappointing.

Figure 7 shows the SGS temperature dissipation profiles. LES values are lower than those of exact values but the overall shape of the profiles is generally similar. This suggests that energy transfer between resolved and subgrid-scales are predicted better than SGS heat flux vectors regardless of accuracy of SGS heat flux. The nature of the QUICK scheme used in solving the equation (3) is likely to damp out the temperature fluctuations. This would subsequently influence to the calculations of q_k and ε_q . Presently, how much the QUICK scheme affects the SGS terms is not known when a box filter is used and thus the results presented in Figs. 6-7 should be interpreted with caution.

If the Reynolds number is large and the molecular Prandtl number is close to 1, one expects that the energy spectra of temperature variance show inertial and viscous-dissipation subranges. However, as the Prandtl number becomes larger (say, $Pr \gg 1$), several distinct subranges will appear. Firstly, there is an appreciable part of the spectrum where the thermal diffusivity is unimportant. This is called the inertial-convective subrange in which temperature fluctuations are simply convected. The second region is the viscous-convective range where viscosity becomes important at wave numbers where the thermal diffusivity does not yet affect the temperature spectrum. Finally, there exist a region called viscous-diffusive subrange where both viscosity and thermal diffusivity become active. If the spirit of LES lies in utilizing large, energy-containing scales to model the SGS scales, one needs to clarify how having grid and test filter widths in the energy-containing, inertial-convective, viscous-convective, viscous-diffusive ranges of the energy spectrum of the temperature field affects the accuracy

of the numerical results. This remains as a future work but it should be analyzed at much higher Reynolds number in order to have well-defined

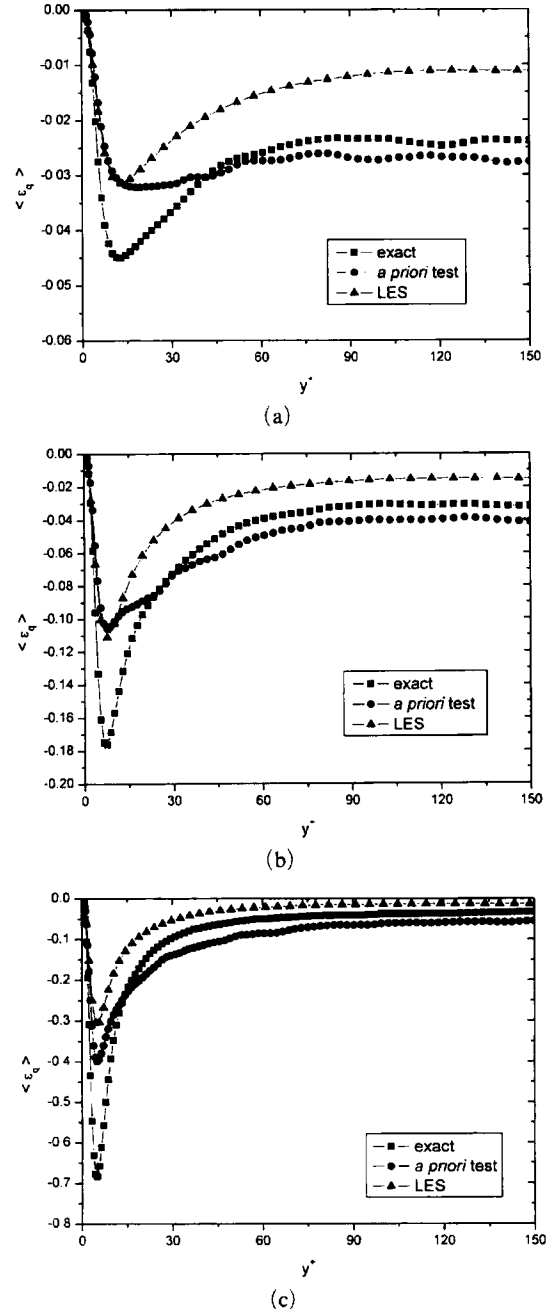


Fig. 7 Plane-averaged subgrid-scale temperature dissipation, $\langle \varepsilon_q \rangle$ (a) $Pr=1$; (b) $Pr=3$; (c) $Pr=10$

subranges. In the present study, the smaller filter width (or equivalently higher resolution) was used for $Pr=10$ based on Fig. 2 but any attempt to access how much SGS contribution results from the given filter width for a given Prandtl number was not made.

Cabot and Moin (1993) have analyzed the DNS data of Rogers et al. (1986) for passive scalars with Prandtl number of 0.2, 0.7, 2.0 and showed that the SGS turbulent Prandtl number, $Pr_{t,SGS} = C/C_T$, tends to have the values between 0.4-0.6 in the middle of the channel and the result is rather insensitive to the filter width. It is not expected that values of the SGS and full-field turbulent Prandtl number are the same as they are derived from different spatial scales due to the filtering operation. Turbulent Prandtl number at SGS level, $Pr_{t,SGS}$ presented in Fig. 8 shows large statistical fluctuation. As more samples are added, it gets smoother although slowly, but the overall shapes hardly change. Thus, it was decided not to continue the simulation in the interest of saving computational resources since it is reasonably acceptable for the purpose of *a priori* test as mentioned in section 2.2. At or in the vicinity of the wall, $Pr_{t,SGS}$ from the filtered DNS field rises to a value around 1.47 for $Pr=10$ and remains higher than that of LES for the most of the channel except in the near-wall region. The best agreement is obtained for $Pr=3$ and the LES result overestimates in the case of $Pr=1$. Thus,

this is the indication that the DSM for scalar transport does not provide accurate values of SGS diffusivity for $Pr=1$ and 10. As mentioned earlier, for the case of $Pr=10$, wider range of scales may appear in the energy spectra (if the Reynolds number is high enough) and the effect of filter width on the results should be further analyzed in the future work.

4. Summary

The dynamic SGS diffusivity approach for passive scalar of Cabot and Moin (1993) has been applied to much higher Prandtl number flows (Pr up to 10). *A priori* test using DNS data indicates that the prediction of SGS heat flux and temperature dissipation give less satisfactory results than in the prediction of SGS stress and dissipation as the Prandtl number becomes larger. However, the shape of SGS temperature dissipation profiles shows a reasonable agreement between the exact and LES results and, perhaps, this would tell why the DSM gives an acceptable mean temperature field mainly because the energy transfer between resolved and subgrid-scales are reasonably simulated even though prediction of SGS heat flux is unsatisfactory. On the other hand, its success of DSM in the prediction of low Reynolds number flows may be attributed to the fact that it acts as a damping function for the eddy viscosity and diffusivity in the wall region as the test filter width is usually located in the inertial range and a grid filter width is in the dissipation range as argued by Orszag et al. (1993).

A priori test suggests that the SGS turbulent Prandtl number can depend on molecular Prandtl number. Since the LES results do not show the sensitivity to Prandtl number away from the wall, this indicates that the DSM for scalar transport does not provide an accurate value of SGS diffusivity for the Prandtl numbers considered.

In the light of the present analysis, the range of applicability of the DSM in its current form will be limited in the prediction of mean temperature and root-mean square fluctuations as the Prandtl number becomes larger. More effort in modelling

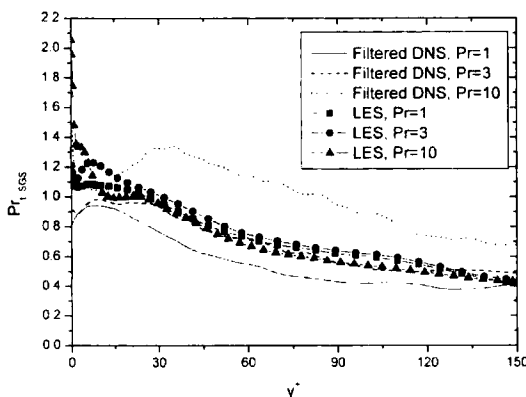


Fig. 8 Subgrid-scale turbulent Prandtl number from *a priori* test and LES

work such as an investigation of properties of the DSM using different types of filter or analysis of the flows where the Reynolds number is high enough to have well-defined ranges in the energy spectra should be made for the high Prandtl (or Schmidt) number flows.

Acknowledgment

This work was supported by Korea Research Foundation Grant (KRF-2000-003-E00012).

References

- Cabot, W. and Moin, P., 1993, "Large Eddy Simulation of Scalar Transport with the Dynamic Subgrid-Scale Model," in *Large Eddy Simulation of Complex Engineering and Geophysical Flows*, ed. B. Galperin and S. A. Orszag, Cambridge University Press.
- Clark, R. A., Ferziger, J. H. and Reynolds, W. C., 1979, *J. Fluid Mech.*, Vol. 91, p. 1.
- Erlebacher, G., Hussaini, M. Y., Speziale, C. G. and Zang, T. A., 1990, "Toward the Large-eddy Simulation of Compressible Turbulent Flows," ICASE Rep. 90-76, NASA/Langley Research Center.
- Germano, M., Piomelli, U., Moin, P. and Cabot, W. 1991, "A Dynamic Subgrid-Scale Eddy Viscosity Model," *Phys. Fluids A* 3(7), pp. 1760~1765.
- Ghosal, S., 1996, "An Analysis of Numerical Errors in Large Eddy Simulations of Turbulence," *J. Comput. Physics*, Vol. 125, pp. 187~206.
- Kasagi, N., Tomita, Y. and Kuroda, A., 1992, "Direct Numerical Simulation of Passive Scalar Field in a Turbulent Channel Flow," *ASME J. Heat Transfer*, Vol. 114, pp. 598~606.
- Kim J., Moin, P. and Moser, R., 1989, "Turbulence Statistics in Fully Developed Channel Flow at Low Reynolds Number," *J. Fluid Mech.*, Vol. 177, pp. 133~166.
- Lilly, D. K., 1992, "A Proposed Modification of the Germano Subgrid-Scale Closure Method," *Phys. Fluids, A* 4, pp. 633~635.
- Na, Y., Papavassiliou, D. V. and Hanratty, T. J., 1999, "Use of Direct Numerical Simulation to Study the Effect of Prandtl Number on Temperature Fields," *Int. J. Heat Fluid Flow*, Vol. 20, pp. 187~195.
- Orszag, S. A., Staroselsky, I. and Yakhot, V. Y., "Some Basic Challenges for Large Eddy Simulation Research," in *Large Eddy Simulation of Complex Engineering and Geophysical Flows*, ed. by B. Galperin and S. A. Orszag, Cambridge University Press.
- Piomelli, U., Cabot, W., Moin, P. and Lee, S., 1991, "Subgrid-scale Backscatter in Turbulent and Transitional Flow," *Phys. Fluids, A* 3(7), pp. 1766~1771.
- Rogers, M., Moin, P. and Reynolds, W. C., 1986, "The Structure and Modeling of the Hydrodynamic and Passive Scalar Fields in Homogeneous Turbulent Shear Flow," Rep. TF-25, Stanford University, Dept. of Mechanical Engineering.
- Spalart, P. R., Moser, R. D. and Rogers, M., 1991, "Spectral Methods for the Navier-Stokes Equations with One Infinite and Two Periodic Directions," *J. Comput. Phys.*, Vol. 96, pp. 297~324.
- Subramanian, C. S. and Antonia, R. A., 1981, "Effect of Reynolds Number on a Slightly Heated Turbulent Boundary Layer," *Int. J. Heat Mass Trans.*, Vol. 24(11), pp. 1833~1846.
- Vreman, B., Geurts, B. and Kuerten, H., 1997, "Large Eddy Simulation of the Turbulent Mixing Layer," *J. Fluid Mech.*, Vol. 339, pp. 357~390.